Theor Chim Acta (1993) 86: 391–416

Theoretica Chimica Acta

Comparison of the Hartree–Fock, Møller–Plesset, and Hartree–Fock–Slater method with respect to electrostatic properties of small molecules

Effects of electron correlation

Guus J. M. Velders and Dirk Feil

Chemical Physics Laboratory, University of Twente, PO Box 217, NL-7500 AE Enschede, The Netherlands

Received December 21, 1992/Accepted February 17, 1993

Summary. The results of various quantum chemical calculations, the Hartree–Fock (HF) method, the Møller–Plesset perturbation theory (MP2), and the Hartree–Fock–Slater (HFS) method are compared. Atomic charges, dipole moments, topological properties of the electron density distribution and polarizabilities, and first hyperpolarizabilities are calculated. Atomic charges obtained with the HFS method are found to be very close to those calculated with the MP2 method, from which we conlcude that the HFS method describes to some extent electron correlation effects. Performing an MP2 calculation after an HF calculation improves the molecular dipole moments considerably, yielding values close to the experimental ones. HFS calculations are computationally less demanding than MP2 and yield comparable results for the electron density distributions, dipole moments and polarizabilities.

Key words: Electron correlation – Atomic moments – Electron density distribution – (Hyper)polarizability – $X\alpha$ versus Møller–Plesset perturbation theory

1 Introduction

The results obtained with different quantum chemical methods, Hartree–Fock (HF), Møller–Plesset perturbation theory (MP2), and Hartree–Fock–Slater (HFS), will be compared. The molecules we use for this study are formaldehyde, water, nitrate ion, and urea. To obtain a good overall picture, the methods will be evaluated using different approaches: electron density maps, atomic moments, topological analysis, and polarizabilities.

We have calculated electron density maps and investigated the influence of the basis set size. Quantitative comparisons have been carried out by evaluating atomic charges and dipole moments. The Mulliken, Löwdin, Hirshfeld stockholder, and Bader charge partitioning methods are employed. The topology of the electron density distribution is very important in Bader's theory of atoms in molecules. Topological analyses have been performed and the properties at the critical points of the electron density distributions will be discussed.

Related to the electron density distribution are the dipole moment, dipole polarizability, and first dipole hyperpolarizability. These properties have been

calculated for formaldehyde using extensive basis sets and the results of the different types of calculations will be compared mutually and with experimentally obtained values.

It is generally assumed that some electron correlation effects are taken into account in density functional methods. Geometries and spectroscopic properties are often predicted more accurately using density functional methods, than using HF. It is well known, for example, that H_2 dissociates correctly into neutral atoms using the HFS (or $X\alpha$) method, while electron correlation corrections must be applied to the HF method to obtain the same result. Cook and Karplus [1] explained the different behavior of the HFS and HF method on dissociation of molecules. They showed that in molecules, within the single determinant HF approximation, the presence of state- and geometry-dependent ionic errors, relative to the correct HF description of the individual free atoms constituting the molecule, are responsible for most of the error in the HF potential surface. This is specially true at large bond distances. These errors are not present in the density and will therefore also be absent in density functional methods.

We will compare HFS and MP2 results and pay special attention to the idea of electron correlation effects in the electron density distribution obtained by both methods.

2 Computational methods

The three quantum chemical methods we used for calculating the propeties of the molecules are the restricted Hartree–Fock (HF) method, the Hartree–Fock–Slater (HFS) method (see Sect. 2.1), and Møller–Plesset perturbation theory (MP2) (see Sect. 2.2).

2.1 The Hartree–Fock–Slater method

The Density Functional Theory [2] (DFT) as formulated by Hohenberg and Kohn [3] states that the ground state electron density distribution $\varrho(r)$ fully characterizes all properties of a system. Although a unique way to derive the ground state energy, wavefunction and related properties, is not known, they can in principle all be determined from knowledge of $\varrho(r)$. In this method, as in the HF method, the N-electron problem is reduced to a set of one-electron equations describing the behavior of one particle in a mean potential field. This field is in the DFT a functional of $\varrho(r)$.

In the Hohenberg–Kohn–Sham formalism [3, 4], the calculation for spin restricted states thus consists of self-consistently solving:

$$[-\tfrac{1}{2}\nabla^2 + V_{\text{eff}}(r)]\phi_i(r) = \varepsilon_i\phi_i(r) \tag{1}$$

where

$$V_{\text{eff}}(r) = \sum_n \frac{Z_n}{|r - R_n|} + \int \frac{\varrho(r')}{|r - r'|}\,dr' + V_{xc}(r) \tag{2}$$

(i.e. the sum of the nuclear potential acting on the electrons, the Coulomb potential produced by all the electrons and the exchange-correlation potential).

The ground state electron density distribution $\varrho(r)$ is given by:

$$\varrho(r) = \sum_i n_i |\phi_i(r)|^2 \tag{3}$$

in which n_i is the occupation number of the orbital ϕ_i. The exchange-correlation potential $V_{xc}(r)$ is in the local density or HFS version approximated by:

$$V_{xc}(r) = -3\alpha \left[\frac{3}{8\pi} \varrho(r) \right]^{1/3} \tag{4}$$

where α is an adjustable parameter, taken to be 0.7 in the present work.

In the $X\alpha$-LCAO-DVM method as developed by Baerends, Ellis, and Ros [5, 6], the orbitals ϕ_i are expanded in a finite set of Cartesian Slater-type orbitals (STO) centered on the atoms: Linear Combination of Atomic Orbitals (LCAO) method. In the Hartree–Fock method a number of two-electron integrals proportional to N_χ^4 have to be calculated, where N_χ is the number of basis functions. To avoid the calculation of this large number of integrals, the electron density distribution $\varrho(r)$ is expanded in a finite set of STO's f_i centered on the nuclei:

$$\varrho(r) \simeq \tilde{\varrho}(r) = \sum_i a_i f_i(r). \tag{5}$$

The coefficients a_i are determined by minimizing the error function:

$$D = \int [\varrho(r) - \tilde{\varrho}(r)]^2 \, dr, \tag{6}$$

with a constraint on the total number of electrons N:

$$\int \varrho(r) \, dr = N. \tag{7}$$

The fit functions f_i are generated by making products of the atomic basis set functions. The fit density $\tilde{\varrho}(r)$ is used to calculate both the Coulomb and exchange-correlation potential. The matrix elements in the secular equation are evaluated numerically according to the Discrete Variational Method (DVM) as introduced by Ellis and Painter [7, 8]. The numerical integrations have been performed by using Gauss–Legendre quadrature [9].

2.2 Møller–Plesset perturbation theory

Electron correlation [10–13] is defined as the difference between the exact solution of the total non-relativistic Hamiltonian of a system, within the Born–Oppenheimer approximation, and the approximated solution in the HF limit. It reflects the fact that the Hartree–Fock Hamiltonian contains the average, rather than the instantaneous potential, and thus neglects the correlation between the motion of the electrons. Apart from this there are also correlation effects related to relativistic effects and nuclear motion which will not be considered here.

The expectation value of a single particle operator, like the charge density distribution and the dipole moment, will be constructed in the general case of a multideterminental wavefunction. Møller–Plesset perturbation theory [14–16] uses the HF wavefunction as a starting point and, in the spin unrestricted case (UHF).

In general all possible substitutions have to be considered but often only the terms containing single and double substitutions of the ground state HF wavefunctions are incorporated in the wavefunction expansion, since for an energy calculation only the double substitutions mix with the ground state. Including only these terms the wavefunction can be written in general as:

$$\psi = N_N(\psi_0 + C_S\psi_S + C_D\psi_D) \tag{8}$$

in which $C_S\psi_S$ and $C_D\psi_D$ represent all terms with single and double substitutions respectively, with respect to ψ_0. The factor N_N takes care of the normalization. The expectation value of a one-electron operator becomes:

$$A = \langle\psi|\hat{A}|\psi\rangle = N_N^2(\langle\psi_0|\hat{A}|\psi_0\rangle + 2C_S\langle\psi_0|\hat{A}|\psi_S\rangle + C_{D1}C_{D2}\langle\psi_{D1}|\hat{A}|\psi_{D1}\rangle + 2C_SC_D\langle\psi_S|\hat{A}|\psi_D\rangle + C_{S1}C_{S2}\langle\psi_{S1}|\hat{A}|\psi_{S2}\rangle). \tag{9}$$

Using MP perturbation theory it follows that, in terms of the perturbation parameter λ, C_D is a first-order perturbation coefficient $O(\lambda)$ while C_S is of second-order $O(\lambda^2)$. Therefore only the first three terms in Eq. (9) have to be kept to obtain the expectation value of the one-electron operator $\hat{A}$ accurate up to second-order in the perturbation theory parameter. For this reason it is not necessary to include triple and higher substitutions in the wavefunction, Eq. (8), since these will not contribute to the second-order Møller–Plesset perturbation theory (MP2), which we are interested in. It is clear from Eq. (9) that single substitutions contribute to the expectation value of the dipole moment and charge density distribution up to second-order, while they don't contribute to the second-order Møller–Plesset calculation of the energy.

The expectation value of $\hat{A}$ can be expressed in two terms: one coming from the first-order perturbation (double substitutions) and one coming from the second-order (single substitutions):

$$\Delta A_{\mathrm{MP2}} = A_{\mathrm{MP2}} - A_{\mathrm{SCF}} = \frac{C_D^2}{1+C_D^2}(A_{\mathrm{SCF}} + A_{D1D2}) + \frac{2C_S}{1+C_D^2}(A_{0S}). \tag{10}$$

The contribution to the electron correlation is ΔA_{MP2}, the difference between the total value (A_{MP2}) and the HF value (A_{SCF}).

For explicit expressions of the coefficients C_S and C_D we refer to [15, 16]. We used the program package GAMESS [17, 18] to calculate the HF wavefunction and perform a MP perturbation calculation to obtain the second-order correction to the energy. The program was modified to calculate all the two-electron integrals needed, including the terms coming from single substituted wavefunctions, which don't have to be calculated for the second-order energy correction. The two-electron integrals are used in other programs to calculate the coefficients C_S and C_D. From these coefficients the density matrix is calculated, from which the electron density distribution and multipole moments can be obtained.

2.3 Electron density distributions

The electron density distributions derived from these methods are named as follows:

$\varrho_{\mathrm{HF}}(r)$: Total electron density distribution from a Hartree–Fock (HF) calculation.

$\varrho_{\mathrm{HFS}}(r)$: Same as above for a Hartree–Fock–Slater ($X\alpha$) calculation.

$\Delta\varrho_{\mathrm{HF}}(r) = \varrho_{\mathrm{HF}}(r) - \sum \varrho_i^{\mathrm{atom}}(r)$: electron deformation (or difference) density distribution. The free spherical atom densities have been calculated using the same atomic basis set as in the molecular calculation.

$\Delta\varrho_{\mathrm{HFS}}(r) = \varrho_{\mathrm{HFS}}(r) - \sum \varrho_i^{\mathrm{atom}}(r)$: electron deformation density distribution. All terms have been calculated using the same atomic basis set.

$\Delta\varrho_{\mathrm{MP2}}(r)$: Difference between the total Møller–Plesset (MP2) electron density distribution and the HF density $\varrho_{\mathrm{HF}}(r)$.

From the calculated wavefunctions Mulliken and Löwdin atomic charges are determined, while the partitioning methods of Hirshfeld (Sect. 2.4) and Bader (Sect. 2.5) have been applied to the different electron density distributions to obtain atomic charges and local atomic dipole moments. For comparing total electron density distributions critical points have been determined and the molecular properties at these critical points according to Bader's theory of "atoms in molecules".

2.4 Hirshfeld's charge partitioning method

To obtain quantitative information from the electron density distribution atomic charges and multipole moments can be calculated. Since there is no unique way to define atomic charges several methods [19] are in use. Very popular from the quantum chemical point of view is the Mulliken [20, 21] partitioning method to analyze a LCAO-MO-SCF wavefunction. Unfortunately, Mulliken atomic charges as well as the Löwdin [22] atomic charges are quite sensitive for the basis set used in the calculation.

The Hirshfeld [23] stockholder partitioning method is closely related to the definition of the promolecule, i.e. the sum of the electron density distributions of the free spherical atoms constituting the molecule. In this formalism one defines for each atom a sharing function:

$$W_a(r) = \frac{\varrho_a^{\mathrm{atom}}(r - R_a)}{\sum_b \varrho_b^{\mathrm{atom}}(r - R_b)}, \tag{11}$$

where $\varrho_s^{\mathrm{atom}}(r - R_a)$ is the spherically averaged free atomic density distribution of atom a at position R_a. The sum in the denominator runs over all atoms of the molecule. Using this sharing function the net atomic charges q_a and dipole moments μ_a are calculated from:

$$q_a = -\int W_a(r)\varrho(r)\, dr + Z_a \tag{12}$$

$$\mu_{ai} = -\sum W_a(r)\varrho(r)(r_i - R_{ai})\, dr \tag{13}$$

with similar terms for higher order moments. (The nuclear charge is denoted by Z_a.) Since no analytic expression is available these terms have to be evaluated numerically using Gauss–Legendre quadrature. The advantage of this way of

partitioning is that the atomic charges and multipole moments can be derived from any charge distribution, obtained by theory or experiment. Using this method in quantum chemical calculations, the atomic moments are far less sensitive for the basis set used in the calculation than those obtained with the methods from Mulliken and Löwdin (see also [24]).

2.5 Charge analysis according to Bader

The charge partitioning method discussed before lacks the profound quantum chemical basis present in the method proposed by Bader [25]. His method is based on the topology of the electron density distribution and defines an atom as the union of an attractor, the nucleus, and its associated basin:

$$\nabla\varrho(r) \cdot n(r) = 0, \quad \text{(for all points on the surface)} \tag{14}$$

where n is the vector normal to the surface of the atom. A nucleus acts as an attractor of the $\nabla\varrho(r)$ field; all the trajectories in some neighborhood of a nucleus, its basin, terminate at the nucleus. The trajectories are lines of steepest ascent through the density distribution. A trajectory always stays within the basin in which it originates, i.e. Eq. (14) does not allow trajectories to cross the atomic surface which is therefore also referred to as a zero flux surface. The charge density is characterized by its extrema, or critical points, points at which the gradient vanishes, $\nabla\varrho(r) = 0$. Whether a critical point in $\varrho(r)$ is a maximum or a minimum is determined by the sign of the curvatures (second derivatives) of $\varrho(r)$. The trace of the Hessian matrix of $\varrho(r)$, the second derivative matrix, is called the Laplacian of $\varrho(r)$:

$$\nabla^2\varrho(r) = \left[\frac{\partial^2}{\partial x^2} + \frac{\partial^2}{\partial y^2} + \frac{\partial^2}{\partial z^2}\right]\varrho(r) \tag{15}$$

and is invariant to the choice of coordinate system. The principal axes and corresponding curvatures at the critical point are obtained as the eigenvectors and eigenvalues of the Hessian matrix. The rank of a critical point is denoted by ω and equals the number of non-zero eigenvalues of $\varrho(r)$ at the critical point. The signature σ is the algebraic sum of the signs of the eigenvalues of $\varrho(r)$ at the critical point. A critical point is labelled by the double (ω, σ) [25, 26].

Another way to analyse $\varrho(r)$ is by looking at the Laplacian of $\varrho(r)$. In regions of space where the Laplacian $\nabla^2\varrho(r) < 0$ electronic charge is accumulated and where $\nabla^2\varrho(r) > 0$ electronic charge is depleted, relative to the average of the surrounding points in the density. The advantage of such a visual representation of $\varrho(r)$, compared with the deformation density, is that it is uniquely defined, without a reference function. When comparing densities of different molecules it does not directly yield more information than the intuitively very attractive deformation density.

Another aspect of this theory is that it is possible to characterize atomic interactions [26] using $\varrho(r)$ and the Laplacian of $\varrho(r)$. Atomic interactions fall into two broad classes, shared and closed-shell interactions. In the first class the interaction results from a sharing of charge density between atoms as in covalent and polar bonds. The charge density is contracted towards the region between the nuclei and $\nabla^2\varrho(r)$ at the critical point in the bond is negative, resulting in a large negative value for the potential energy in the internuclear region. The total charge density at the critical point is relatively large.

The characteristics of closed-shell interactions, as found in noble gases, ionic bonds and Van der Waals crystals, are opposite to the shared interactions. Charge is contracted towards the nuclei resulting in a positive Laplacian and a relatively small value of $\varrho(r)$ at the bond critical point. In these interactions the regions of dominant potential energy contributions are separately localized within the boundaries of each interacting atom, while for the shared interactions a region of low potential energy is contiguous over the basins of the atoms participating in the bond.

Properties of the atoms defined by Eq. (14) can be calculated by performing the appropriate integrations [27, 28] over the atomic volumes and surfaces. Because of the complicated definition of the sharp boundary of the atom the calculation of atomic properties is rather complicated and computationally demanding. Interfaces have been written to use the HFS and MP2 wavefunction and density matrices as input for the AIMPAC programs.

2.6 Electric field calculations

To study the influence of electric fields on molecules we have used several methods [29, 30]. The dipole moment μ of a molecule in the presence of a homogeneous electric field E_i, can be represented as a power series expansion in terms of the electric field. Using the summation convention we can write:

$$\mu_i = \mu_{0i} + \alpha_{ij}E_j + \beta_{ijk}E_jE_k + \gamma_{ijkl}E_jE_kE_1 + \cdots \tag{16}$$

where μ_0 is the permanent dipole moment, while the tensors α_{ij}, β_{ijk}, and γ_{ijkl} stand for the dipole polarizability, first dipole hyperpolarizability and second dipole hyperpolarizability, respectively.

2.6.1 The sum over states method: SOS. In this method, which is equivalent to the Uncoupled Hartree–Fock approach (UCHF), a Restricted Hartree–Fock (RHF) calculation is performed with the unperturbed Hamiltonian. Subsequently the influence of an electric field is calculated using perturbation theory [31]. In this method the perturbation ($|e|r \cdot E$) is included in the Fock operator. The dipole (hyper)polarizability can be calculated from a Taylor series expansion of the expectation value of the dipole moment using the perturbed canonical orbitals. The coefficients can also be obtained from the energy expression using the Hellmann–Feynman theorem: The derivative of the energy with respect to the electric field equals the expectation value of the dipole moment. The expressions of the polarizability coefficients a_{ij} and β_{ijk} are given elsewhere [29, 30].

2.6.2 The finite field method: FF. Two versions of this method exist. In the one the calculations are directed towards the calculation of the dipole moment (FF:μ), whereas in the other the energy of the molecule is the object of study (FF:E). In both methods, RHF calculations are performed in the presence of an external electric field. This finite field approach [32, 33] has the advantage over the UCHF method that the perturbation of the orbitals, due to the field, is automatically incorporated in the Fock operator in a self consistent way. The effect of the perturbation of a certain orbital on the other orbitals is not accounted for in the SOS method. The FF method is equivalent in the limit of zero field to the conceptually much more complicated Coupled Hartree–Fock method (CHF). For a comparison between this method and the SOS method see also Velders and Feil [29].

2.6.2.1 The finite field method: FF:μ. The components of the dipole polarizability tensor α_{ij} and first hyperpolarizability tensor β_{ijk} are obtained by numerical differentiation (three point method) of the dipole moment with respect to the electric field components for small fields. Using the MP2 instead of the SCF dipole moments, electron correlation effects are included in the polarizability coefficients. Another way of incorporating electron correlation effects in the (hyper)polarizability is by double perturbation theory calculations [34, 35], in which two perturbations operators are defined. One represents the electron correlation and the other the influence of an external electric field.

2.6.2.2 The finite field method: FE:E. This method is also a finite field method but now the total energy is expanded in a Taylor series in the electric field instead of the dipole moment. The dipole moment, polarizability and first hyperpolarizability are determined from the first, second, and third derivatives of the energy with respect to the electric field components. A numerical five point method is used to calculate these derivatives. For the SCF calculations this method is equivalent to the FF:μ method, but for MP2 it is not. The methods yield different results because with the MP2 dipole moment calculation for FF:μ the perturbation is performed up to second-order in the dipole moment, while calculating FF:E the MP2 energy is accurate up to second-order in the energy. Consequently, with FF:μ both single and double substituted wave functions are taken into account and with FF:E only the double substitutions. We will show that single substitutions give the main electron correlation contribution to the dipole moment so the results of both methods can differ considerably.

It is important to realize that the MP2 calculations are performed using the converged molecular orbitals from the Hartree–Fock calculation in the presence of the field. The effective change in potential caused by electron correlation interactions is not taken into account by using a self-consistent field procedure.

2.7 Basis sets and geometries

For the HF and MP2 calculations we employed the Pople [36–39] basis sets, STO-3G, 4-31G, 6-31G**, and the basis sets of Dunning and Hay [40], TZV, TZV** (TZV = triple zeta valence). The double stars indicate the addition of polarization functions, i.e. an atomic GTO p-functions for the hydrogen atoms and an atomic GTO d-functions for the other atoms [41].

All HFS calculations have been performed using Cartesian STO basis sets. See Table 1 for the exponents used. These basis functions, apart from the polarization functions, have been obtained from a least-squares fit to numerical atomic orbitals from a Herman–Skillman [42] type calculation. The polarization functions were chosen according to the optimizations of Cade and Huo [43], McLean and Yoshimine [44], and Bicerano et al. [45].

The geometrical parameters of the molecules have been optimized by using an HF calculation with a 4-31G basis set (see Table 2). Molecular geometries obtained in this way generally appear to be in good agreement with experiments and extending the basis sets does not significantly improve the geometry [39, 46]. Since the calculated geometry of the water molecule does not agree so well with experiment we used the experimental geometry [47] for our calculations. For the electron density study employed here the molecular geometry is not very important. The same fixed geometry has been used for all calculations described here.

Table 1. Cartesian STO basis sets (STO-type, exponent) used in the Hartree–Fock–Slater calculations. When using a frozen core the 1*s* functions are replaced by a different effective nuclear charge

Basis set	C		H		N		O	
SZV	1*s*	5.30	1*s*	0.85	1*s*	6.38	1*s*	7.36
	2*s*	1.56			2*s*	1.86	2*s*	2.15
	2*p*	1.22			2*p*	1.47	2*p*	1.72
DZV	1*s*	7.68	1*s*	0.76	1*s*	5.90	1*s*	9.80
	1*s*	5.00	1*s*	1.28	1*s*	8.74	1*s*	6.80
	2*s*	1.24			2*s*	2.38	2*s*	2.82
	2*s*	1.98			2*s*	1.45	2*s*	1.70
	2*p*	0.96			2*p*	1.12	2*p*	1.30
	2*p*	2.20			2*p*	2.58	2*p*	3.06
TZV	1*s*	7.68	1*s*	1.58	1*s*	5.90	1*s*	9.80
	1*s*	5.00	1*s*	0.92	1*s*	8.74	1*s*	6.80
	2*s*	1.28	1*s*	0.69	2*s*	1.50	2*s*	1.72
	2*s*	2.10			2*s*	2.50	2*s*	2.88
	2*s*	4.60			2*s*	5.15	2*s*	7.58
	2*p*	0.82			2*p*	1.00	2*p*	1.12
	2*p*	1.48			2*p*	1.88	2*p*	2.08
	2*p*	2.94			2*p*	3.68	2*p*	4.08
TZD = TZV+	3*d*	2.50	2*p*	1.00	3*d*	2.00	3*d*	2.00
TZDF = TZV+	3*d*	2.50	2*p*	1.00			3*d*	2.00
	4*f*	2.00	2*p*	2.00			4*f*	2.50
			3*d*	2.00				

p-functions include: $p_{x,y,z}$
d-functions include: $d_{z^2,x^2-y^2,xy,xz,yz}$
f-functions include $f_{z^3,xz^2,yz^2,xyz,z(x^2-y^2),x(x^2-3y^2),y(3x^2-y^2)}$

Table 2. Molecular geometries, HF(4-31G) optimization

Molecule	Symmetry	Bond length (Å)	Bond angle (degr.)
Formaldehyde[1]	C_{2v}	C–O = 1.2060	O–C–H = 121.82
		C–H = 1.0809	
Water[2,5]	C_{2v}	O–H = 0.9572	H–O–H = 104.52
Nitrate[3]	D_{3h}	N–O = 1.2563	
Urea[3]	C_{2v}	C–O = 1.2268	O–C–N = 122.16
		C–N = 1.3574	C–N–H1 = 117.49
		C–H1 = 0.9898	C–N–H2 = 123.78
		C–H2 = 0.9886	

[1] C(0, 0, 0), O(0, 0, −1.2060), H(0, ±0.9184, 0.5699)
[2] O(0, 0, 0), H(0, ±0.7570, 0.5859)
[3] N(0, 0, 0), O1(0, 0, 1.2558), O2(0, ±1.0876, −0.6279)
[4] C(0, 0, 0), O(0, 0, 1.2268), N(0, ±1.1491, −0.7225), H1(0, ±2.0033, −0.2225), H2(0, ±1.1771, −1.7107)
[5] Experimental geometry [47]. The calculated bond angle HF(4-31G) was too large (111.14°).

3 Results and discussion

3.1 Comparing electron density distributions

Graphs of the electron density distributions calculated with the different methods will be discussed in this section. The molecules we investigated are all planar and only the molecular plane will be considered. To obtain a good overall picture of the density distributions, integrated atomic charges are needed (see Sect. 3.2). The analyses performed in this section are mostly qualitative. The density plots have been calculated using the HF, MP2, and HFS methods.

Boyd and Wang [15, 16] compared density distributions obtained from MP2 and CI (configuration interaction) calculations. Figure 1 is a reprint of their figure of the correlation difference density $\Delta\varrho_{MP2}(r)$ and $\Delta\varrho_{CI}(r)$ of the nitrogen molecule. In both the MP2 and CI calculation only single and double substitutions are taken into account. Meyer et al. [48] showed for CI calculated density distributions that triple and quadruple excitations are only of minor importance. The excellent agreement between the MP2 and CI calculated densities is clearly seen and since the latter method is computationally much more demanding, MP2 density calculations provide a good alternative for studying electron correlation effects.

Before we discuss the different density distribution calculations, some other aspects are considered. In Fig. 2 different plots of the water molecule are shown to investigate the influence of a frozen 1*s* core in the HFS calculations, the influence of extending the basis set and the agreement between atomic HF and HFS calculations. Freezing the 1*s* core on the oxygen atom (Fig. 2b) has only a slight effect on the density distribution (notice the difference in contour intervals) although, because of its dipolar character, it might have some influence on the total dipole moment. Figures 2c (HF) and 2d (HFS) display the effects of using extended basis sets (*f*-functions on the oxygen atom and *d*-functions on the hydrogen atoms) compared to the 6-31G** (HF) and TZD (HFS) basis sets. The extra functions in the basis set are more important for the HFS than for the HF calculations, but in both cases the effects of an extension on the basis set is small compared with the deformation density $\Delta\varrho_{HF}(r)$. Note the small contour intervals in Fig. 2c,d. There are two ways to compare the HF and HFS methods:

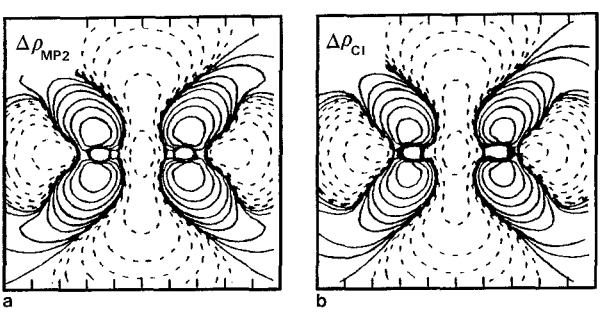

Fig. 1. Correlation difference density plots of the nitrogen molecule N_2. Comparison between MP2 (**a**: $\Delta\varrho_{MP2}(r)$) and CI (**b**: $\Delta\varrho_{CI}(r)$) electron density calculations. ($\Delta\varrho_{CI}(r)$ is defined similar to $\Delta\varrho_{MP2}(r)$). Positive contours are drawn as *solid lines* and negative contours as *dashed lines*. The contour levels are: 0, ±0.0001, ±0.0002, ±0.0005, ±0.001, ±0.002, ±0.005, ±0.01, ±0.02, ±0.05, and ±0.1 a.u. Reprint from Wang and Boyd [15]

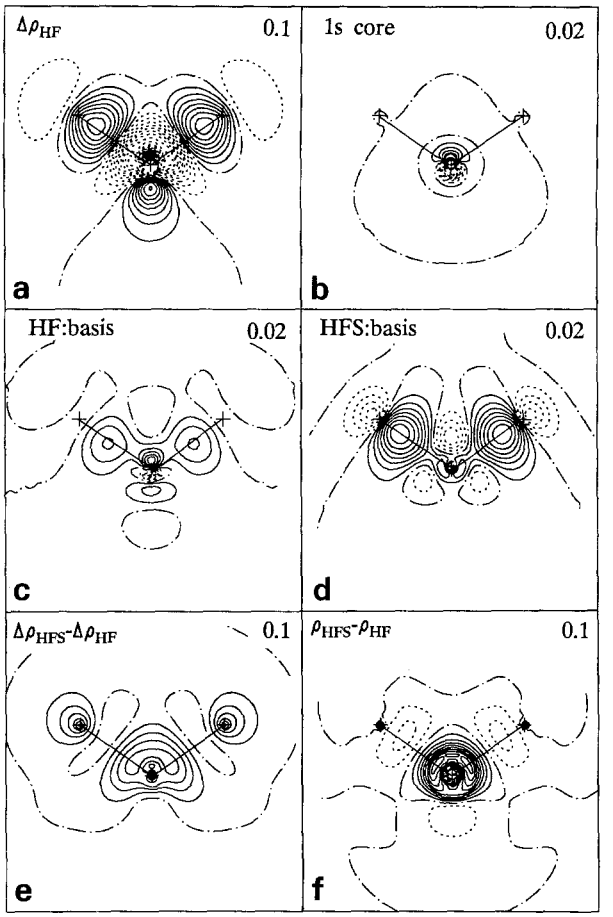

Fig. 2. Electron density plots of the water molecule plotted in the molecular plane. Positive contours are drawn as *solid lines* (electron excess), zero contours are *dash-dotted* and negative contours are *dotted* (electron deficiency). Contour interval 0.10 e/Å^3 for (**a, e, f**) and 0.02 e/Å^3 for (**b, c, d**). **a** Deformation density distribution $\Delta\varrho_{HF}(r)$. **b** Influence of a frozen 1*s* core in the HFS calculation: $\Delta\varrho_{HFS}$(All-electron) $-\Delta\varrho_{HFS}$(frozen 1*s* core oxygen atom). **c** Influence extended basis (*f*-functions on oxygen atom, *d*-functions on hydrogen atoms) for HF calcualtion: $\Delta\varrho_{HF}$(6-31G** + (*f*/*d*)) $-$ $\Delta\varrho_{HF}$(6-31G**); **d** Influence extended basis (*f*-functions on oxygen atom, *d*-functions on hydrogen atoms) for HFS calculation: $\Delta\varrho_{HFS}$(TZD + (*f*/*d*)) $-\Delta\varrho_{HFS}$(TZD). **e** Difference between HFS and HF calculation: $\Delta\varrho_{HFS}(r) - \Delta\varrho_{HF}(r)$. **f** Difference between HFS and HF calculation $\varrho_{HFS}(r) - \varrho_{HF}(r)$

subtracting the deformation density distributions $\Delta\varrho_{HFS}(r) - \Delta\varrho_{HF}(r)$ (Fig. 2e) and subtracting the total densities $\varrho_{HFS}(r) - \varrho_{HF}(r)$ (Fig. 2f). The differences, caused by the difference in the atomic calculations, are largest close to the nuclei. Compared with the property we are investigating, $\Delta\varrho(r)$ (Fig. 2a), the differences in methods of comparison are not insignificant. The advantage of a deformation density is that basis set errors tend to decrease using the same atomic basis set for the calculation of the molecule as for the free atoms. In the following figures the HF and HFS densities are compared using the deformation density distribu-

tions although we realize that some molecular properties are determined by the total densities.

We will now compare electron density distributions calculated with the different quantum chemical methods. The Figs. 3, 4, 5, and 6 show $\Delta\varrho_{HF}(a)$, $\Delta\varrho_{HFS}(b)$, $\Delta\varrho_{MP2}(c)$ and $\Delta\varrho_{HFS} - \Delta\varrho_{HF}(d)$ for formaldehyde, water, the nitrate ion, and the urea molecule, respectively. The basis sets used are the 6-31G** for HF and TZD for HFS. These basis sets are approximately of the same quality. To obtain a good view of the whole range of the molecule logarithmic contour intervals have been used. The overall agreement between the HF and HFS deformation densities is good. The only appreciable difference occurs at the core regions of the nitrogen atoms of the urea. The figures *d* show that the density around the hydrogen atoms is more extended for the HFS calculation than for

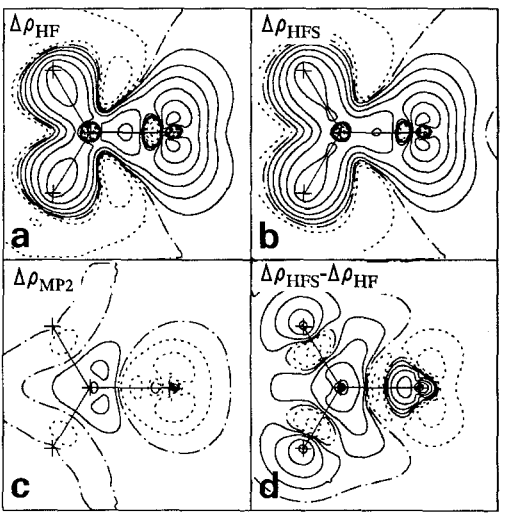

Fig. 3. Electron density plots of the formaldehyde molecule. Basis set HF calculation: 6-31G**, HFS calculation: TZD. Positive contours are drawn as *solid lines*, zero contours are *dash-dotted* and negative contours are dotted. Contour intervals (positive and negative) increase by successive factors of 2 starting from 0.02 e/Å^3. **a** HF deformation density $\Delta\varrho_{HF}(r)$; **b** HFS deformation density $\Delta\varrho_{HFS}(r)$; **c** MP2 contribution to the density $\Delta\varrho_{MP2}(r)$; **d** Difference between HFS and HF density, $\Delta\varrho_{HFS}(r) - \Delta\varrho_{HF}(r)$

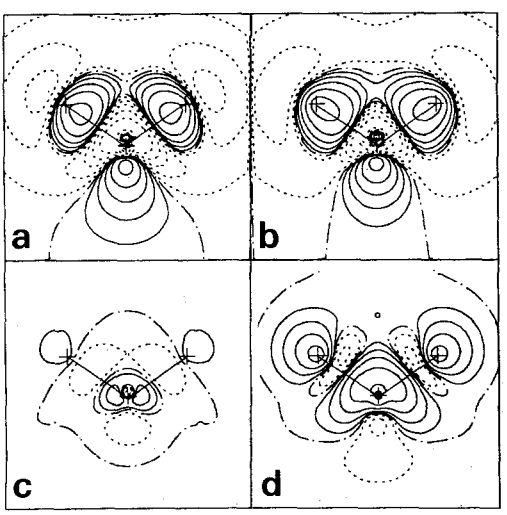

Fig. 4. Electron density plots of the water molecule. Basis set, contours and configuration of the plots as in Fig. 3

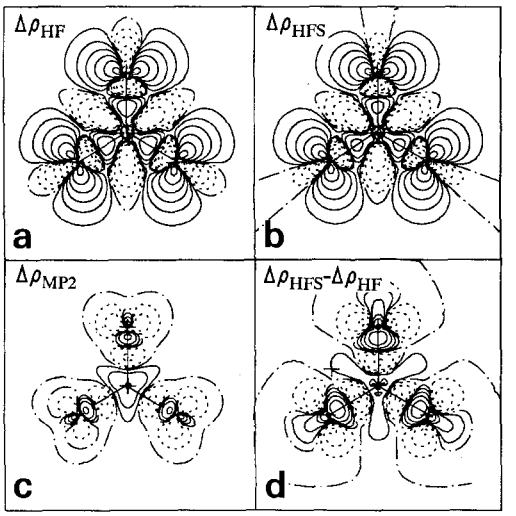

Fig. 5. Electron density plots of the nitrate ion. Basis set, contours and configuration of the plots as in Fig. 3

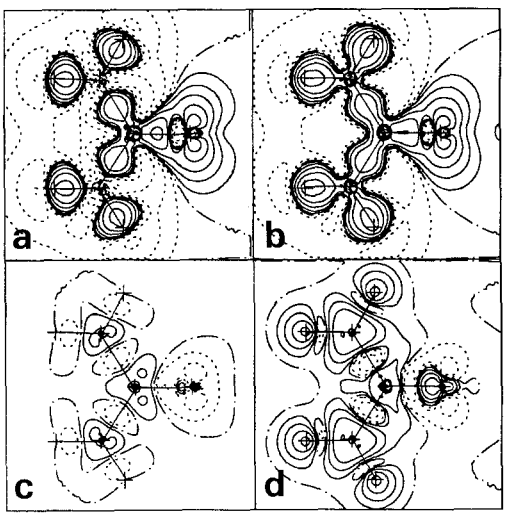

Fig. 6. Electron density plots of the urea molecule. Basis set, contours and configuration of the plots as in Fig. 3

HF. This seems to hold for all molecules. The doubly bonded oxygen atoms show the same pattern in all molecules. The region of electron deficiency in the bond of this atom is deeper in $\Delta\varrho_{HF}$ than in $\Delta\varrho_{HFS}$, while the electron excess in the lone pair region is larger. All features appear to be slightly less pronounced for the HFS than for the HF calculations. When we compare the HFS and HF calculated electron densities with the effect of electron correlation, as shown by the figures *c*, we notice that the HFS method seems to take correlation into account, albeit in a somewhat exaggerated way. This confirms the belief that HFS/DFT accounts to some degree for correlation (see Cook and Karplus [1] and references therein). Qualitatively $\Delta\varrho_{MP2}$ and $\Delta\varrho_{HFS} - \Delta\varrho_{HF}$ behave about the same for all four molecules. Both density maps (*c* and *d*) show negative contours in the bonding areas and positive contours close to the nuclei. At the position of

the characteristic hole in the deformation density of the oxygen atom, both maps show positive features. Because of the different basis sets used in the HF and HFS calculations the figures *c* and *d* cannot be compared quantitatively, but the common features are striking. When comparing the two sets of diagrams it should be remembered that electron correlation effects are also included in the atomic HFS calculations. This last effect is not present when we compare total densities ($\varrho_{HFS} - \varrho_{HF}$) as in Fig. 2*f*. Comparing this kind of figure with $\Delta\varrho_{MP2}$, results in a better agreement for the hydrogen atoms both in and behind the bonds. At the position of the other atoms the agreement is slightly decreased.

From these maps we conclude that the agreement between HF and HFS density distributions is good and that the influence of MP2 contributions is small even compared with the difference between the HF and HFS densities. These figures give obviously only information about the density in molecular plane. In the next section quantitative analysis of atomic moments will be discussed.

3.2 Comparing atomic charges and dipole moments

In Tables 3, 4, 5, and 6 atomic charges are listed calculated with the Mulliken, Löwdin, Hirshfeld, and Bader charge partitioning methods using both HF, MP2, and HFS calculations. In the Hirshfeld partitioning method free spherical atomic densities $\varrho_i^{atom}(r)$ are used in the weight function. For partitioning the HF and MP2 densities the same set of atomic densities has been used; i.e. those derived from atomic Hartree–Fock calculations. This has the advantage that the changes we get in atomic charges can only be caused by changes in the molecular electron density distribution. Atomic charges resulting from MP2 calculations will also be discussed in another paper [49].

Table 3. Atomic charges (in $|e|$) of formaldehyde calculated with the HF, MP2, and HFS methods

Method/basis set		Mulliken	Löwdin	Hirshfeld	Bader
HF/STO-3G	C	0.069	0.077	0.117	1.043
	O	−0.189	−0.113	−0.142	−0.937
	H	0.060	0.018	0.013	−0.053
HF/4-31G	C	0.176	0.123	0.163	0.960
	O	−0.485	−0.282	−0.261	−0.997
	H	0.155	0.080	0.049	0.018
HF/6-31G**	C	0.246	0.081	0.168	1.334[1]
	O	−0.447	−0.259	−0.266	−1.272
	H	0.101	0.089	0.049	−0.031
MP2/6-31G**	C	0.167	−0.002	0.101	1.132[2]
	O	−0.359	−0.169	−0.185	−1.110
	H	0.096	0.085	0.042	−0.011
HFS/TZD	C	0.823		0.098	0.852[3]
	O	−0.451		−0.186	−0.945
	H	−0.186		0.044	0.046

[1] Basis set 6-311G + (2*d*/*pd*): C: 1.228, O: −1.219, H: −0.004.
[2] Basis set 6-311G + (2*d*/*pd*): C: 1.025, O: −1.050, H: 0.012.
[3] Basis set TZV + (2*d*/*pd*): C: 0.915, O: −0.952, H: 0.018.

Table 4. Atomic charges (in $|e|$) of water calculated with the HF, MP2 and HFS, methods

Method/basis set		Mulliken	Löwdin	Hirshfeld	Bader
HF/STO-3G	O	−0.366	−0.253	−0.236	−0.821
	H	0.183	0.127	0.118	0.411
HF/4-31G	O	−0.785	−0.569	−0.332	−0.998
	H	0.393	0.284	0.166	0.499
HF/6-31G**	O	−0.674	−0.454	−0.328	−1.226
	H	0.337	0.227	0.164	0.613
MP2/6 − 31G**	O	−0.647	−0.438	−0.307	−1.162
	H	0.323	0.219	0.153	0.581
HFS/TZD	O	−0.676		−0.306	−1.104
	H	0.338		0.152	0.552

Table 5. Atomic charges (in $|e|$) of the nitrate ion calculated with the HF, MP2, and HFS methods

Method/basis set		Mulliken	Löwdin	Hirshfeld	Bader
HF/STO-3G	N	0.211	0.320	0.286	0.618
	O	−0.404	−0.440	−0.429	−0.539
HF/4-31G	N	0.617	0.496	0.325	0.730
	O	−0.539	−0.499	−0.442	−0.577
HF/6-31G**	N	0.875	0.456	0.320	0.960
	O	−0.625	−0.486	−0.440	−0.653
MP2/6-31G**	N	0.724	0.307	0.203	0.778
	O	−0.575	−0.436	−0.401	−0.593
HFS/TZD	N	0.592		0.172	0.842
	O	−0.531		−0.391	−0.614

We first consider the basis set dependence of HF calculated atomic charges. There is a strong basis set dependence for both the Mulliken, Löwdin and Bader atomic charges. For the first two this basis set dependence is explicitly present in the partitioning method itself, while for Bader's method small changes in the position of the sharp boundaries of the atoms can result in considerable changes in the various moments. The atomic charges according to Hirshfeld show a much more consistent behavior. The values calculated with a 6-31G** basis set hardly differ from the 4-31G values. This makes the Hirshfeld atomic charges better suited for comparing the outcome of different quantum chemical calculations than the other partitioning methods. Experience shows that for Bader atomic charges a 6-31G** basis set does give consistent results; increasing the basis set does not cause large changes (see the bottom of Table 3 for calculations with larger basis sets and see also [25, 26]).

The magnitude of the atomic charges according to Bader are clearly much larger than all others, while Hirshfeld's method usually yields the smallest values. For comparing different calculations or molecules this is not important, but in modelling molecules it does matter which set of charges is used. Davidson and Chakravorty [24] compared Mulliken, Löwdin, and Hirshfeld atomic charges

Table 6. Atomic charges (in $|e|$) of urea calculated with the HF, MP2, and HFS methods

Method/basis set		Mulliken	Löwdin	Hirshfeld	Bader
HF/STO-3G	C	0.428	0.312	0.290	2.158
	O	−0.341	−0.311	−0.317	−1.101
	N	−0.461	−0.283	−0.212	−1.211
	H1	0.216	0.147	0.116	0.353
	H2	0.201	0.135	0.110	0.329
HF/4-31G	C	1.028	0.406	0.272	1.749
	O	−0.676	−0.467	−0.420	−1.130
	N	−0.931	−0.460	−0.178	−1.136
	H1	0.390	0.254	0.130	0.430
	H2	0.364	0.236	0.122	0.396
HF/6-31G**	C	0.940	0.301	0.255	2.507
	O	−0.657	−0.438	−0.419	−1.415
	N	−0.772	−0.334	−0.172	−1.472
	H1	0.328	0.211	0.132	0.482
	H2	0.302	0.191	0.122	0.444
MP2/6-31G**	C	0.810	0.195	0.175	2.188
	O	−0.567	−0.349	−0.343	−1.270
	N	−0.735	−0.320	−0.166	−1.356
	H1	0.320	0.209	0.130	0.468
	H2	0.294	0.189	0.120	0.429
HFS/TZD	C	0.771		0.183	1.590
	O	−0.602		−0.318	−1.061
	N	−0.106		−0.200	−1.090
	H1	0.021		0.139	0.429
	H2	0.001		0.128	0.397

and dipole moments for a large number of molecules and found similar results for the basis set dependence as reported here.

We will now compare atomic charges calculated with the HFS method with HF calculated values. Comparing the HFS calculated charges with the HF/6-31G** values there does not appear to be a uniform pattern. The differences between HFS and HF charges are of the same order of magnitude, or larger than the differences caused by changes in the basis sets. The best agreement occurs when the Hirshfeld partitioning method is applied. Part of this may be caused by the fact that these charges are smaller in magnitude than the others. The most consistent behavior can be seen for the Hirshfeld charges of the hydrogen atoms which are almost equal for both methods.

The effect of electron correlation on atomic charges will now be considered. For all the atoms in the different molecules and all partitioning methods we used, the MP2 method yields lower atomic charges than the HF method; electron correlation reduces the atomic charges. The MP2 correlation on the density plots was seen to be small compared with the difference between the HFS and HF densities, but the MP2 correction is seen to affect the atomic charges considerably. There is an excellent agreement for all molecules between the MP2 and HFS atomic charges using Hirshfeld's method. With the Bader partitioning method not such a good agreement is found, although the MP2 charges are always lying between the HF and HFS calculated values. Larger basis sets

(bottom of Table 3) yield a slightly better agreement between the MP2 and HFS calculated charges. This again confirms the suggestion that the HFS method yields electron densities beyond Hartree–Fock quality. Because a completely different type of basis set is used in the HF (and MP2) method and in the HFS method, a comparison of Mulliken atomic charges is hardly relevant. As has been emphasized before the method of Bader is sensitive to small changes in the density caused by different methods or basis sets. This phenomenon is probably responsible for the larger differences between both methods than found using Hirshfeld's partitioning method.

For quantifying electron density distributions the higher moments should be considered as well. Tables 7 and 8 list the local atomic dipole moments using the

Table 7. Atomic dipole moments (in a.u.) using Hirshfeld stockholder partitioning method. The central bond of the molecules (C=O, N–O1) is directed along the z-axis, while the molecules are lying in the y-z plane. The atoms marked with a (′) are located on the negative y-axis (see Table 2). The basis sets used are HF, MP2: 6-31**, HFS: TZD

		HF		MP2		HFS	
		μ_{yi}	μ_{zi}	μ_{yi}	μ_{zi}	μ_{yi}	μ_{zi}
Formaldehyde	C	0.000	−0.097	0.000	−0.076	0.000	−0.071
	O	0.000	−0.148	0.000	−0.138	0.000	−0.075
	H	0.093	−0.070	0.091	−0.067	0.149	−0.096
	H′	−0.093	−0.070	−0.091	−0.067	−0.149	−0.096
	$\sum \mu_i$	0.000	−0.384	0.000	−0.347	0.000	−0.338
	μ_{mol}^{1}	0.000	−1.095	0.00	−0.858	0.000	−0.854[2]
Water	O	0.000	0.202	0.000	0.206	0.000	0.069
	H	0.175	0.147	0.168	0.141	0.219	0.150
	H′	−0.175	0.147	−0.168	0.141	−0.219	0.150
	$\sum \mu_i$	0.000	0.497	0.000	0.487	0.000	0.369
	μ_{mol}	0.000	0.859	0.000	0.826	0.000	0.707[3]
Nitrate	N	0.000	0.000	0.000	0.000	0.000	0.000
	O1	0.000	−0.256	0.000	−0.242	0.000	−0.231
	O2	−0.221	0.128	−0.209	0.121	−0.200	0.116
	O2′	0.221	0.128	0.209	0.121	0.200	0.116
	$\sum \mu_i$	0.000	0.000	0.000	0.000	0.000	0.000
	μ_{mol}	0.000	0.000	0.000	0.000	0.000	0.000
Urea	C	0.000	−0.088	0.000	−0.087	0.000	−0.084
	O	0.000	−0.205	0.000	−0.187	0.000	−0.138
	N	−0.014	0.008	−0.005	0.001	−0.009	0.002
	N′	0.014	0.008	0.005	0.001	0.009	0.002
	H1	0.187	0.097	0.181	0.091	0.232	0.100
	H1′	−0.187	0.097	−0.181	0.091	−0.232	0.100
	H2	0.011	−0.203	0.011	−0.195	0.022	−0.246
	H2′	−0.011	−0.203	−0.011	−0.195	−0.022	−0.246
	$\sum \mu_i$	0.000	−0.490	0.000	−0.479	0.000	−0.509
	μ_{mol}	0.000	−1.888	0.000	−1.703	0.000	−1.644[4]

[1] Dipole moment of the molecule.
[2] Experimental values −0.917 a.u. [50] and −0.920 a.u. [51].
[3] Experimental values 0.763 a.u. [51], 0.7296 a.u. [52], 0.728 a.u. [53], 0.7268 a.u. [54].
[4] Experimental value −1.51 a.u. [55].

Table 8. Atomic dipole moments (in a.u.) using the partitioning method of Bader. For specifications of the calculations and experimental values see Table 7

		HF		MP2		HFS	
		μ_{yi}	μ_{zi}	μ_{yi}	μ_{zi}	μ_{yi}	μ_{zi}
Formaldehyde	C	0.000	0.877	0.000	0.875	0.000	0.858
	O	0.000	0.739	0.000	0.620	0.000	0.320
	H	−0.092	0.060	−0.109	0.076	−0.139	0.110
	H′	0.092	0.060	0.109	0.076	0.139	0.110
	$\sum \mu_i$	0.000	1.736	0.000	1.646	0.000	1.399
	μ_{mol}	0.000	−1.095	0.000	−0.858	0.000	−0.854
Water	O	0.000	−0.309	0.000	−0.255	0.000	−0.286
	H	−0.123	−0.095	−0.131	−0.103	−0.131	−0.114
	H′	0.123	−0.095	0.131	−0.103	0.131	−0.114
	$\sum \mu_i$	0.000	−0.498	0.000	−0.460	0.000	−0.515
	μ_{mol}	0.000	0.859	0.000	0.826	0.000	0.707
Nitrate	N	0.000	0.000	0.000	0.000	0.000	0.000
	O1	0.000	−0.374	0.000	−0.388	0.000	−0.438
	O2	−0.324	0.187	−0.336	0.194	−0.379	0.219
	O2′	0.324	0.187	0.336	0.194	0.379	0.219
	$\sum \mu_i$	0.000	0.000	0.000	0.000	0.000	0.000
	μ_{mol}	0.000	0.000	0.000	0.000	0.000	0.000
Urea	C	0.000	0.106	0.000	0.133	0.000	0.199
	O	0.000	0.657	0.000	0.562	0.000	0.192
	N	0.226	−0.152	0.134	−0.094	0.000	0.109
	N′	−0.226	−0.152	−0.134	−0.094	0.000	0.109
	H1	−0.143	−0.078	−0.148	−0.081	−0.155	−0.083
	H1′	0.143	−0.078	0.148	−0.081	0.155	−0.083
	H2	−0.005	0.171	−0.006	0.178	−0.009	0.190
	H2′	0.005	0.171	0.006	0.178	0.009	0.190
	$\sum \mu_i$	0.000	0.646	0.000	0.700	0.000	0.823
	μ_{mol}	0.000	−1.888	0.000	−1.703	0.000	−1.644

Hirshfeld and Bader partitioning methods. For most atoms the agreement between the HF and HFS calculations is reasonable, while the MP2 correction on the atomic dipole moments is small. This holds for both partitioning methods although they yield quite different values. The local dipole moments calculated with Bader's method are large because the nuclei are in general not located in the center of the atomic basins. Charge transfer yields for Hirshfeld's method the most important contributions to the molecular dipole moment, while the contribution of the atomic dipole moments has the same direction but is of less importance. Bader's partitioning method shows large charge transfer between the atoms. The resulting molecular dipole moments are reduced by the oppositely directed atomic dipole moments.

The HFS calculated molecular dipole moments are closer to the experimental values than the ones calculated with the HF method. For formaldehyde MP2 yields a dipole moment in excellent agreement with experiment (see also Sect. 3.4) but for water the MP2 contribution is small ($\mu_{\text{MP2}} = 0.8264$ a.u.). Using a

TZDF basis set Krijn and Feil [56] calculated an HFS dipole moment of 0.721 a.u. even closer to the experimental values.

3.3 Critical points

In this section we compare the electron density distributions by means of the properties at the critical points in the molecular bonds. Table 9 lists the electron density $\varrho(r_c)$ and the Laplacian of the electron density $\nabla^2\varrho(r_c)$. The basis set dependence of r_c and $\varrho(r_c)$ is not large and the HFS values are in reasonable agreement with the HF/6-31G** values. The agreement increases taking electron correlation effects into account, although the MP2 calculations yield almost the same results as the HF calculations. From the density plots, Figs. 3c t/m 6c, follows that $\Delta\varrho_{MP2}$ is positive at the bond critical point in the C=O bond of formaldehyde and negative in all other bonds [26]. Although the MP2 contribution to the density, $\Delta\varrho_{MP2}(r)$, was seen to be small in the density plots, Sect. 3.1, for the density in the bonds it is significant. For almost all calculated values of r_c, $\varrho(r_c)$, and $\nabla^2\varrho(r_c)$ it can be seen that the MP2 values are lying between the HF and HFS values. This again shows that HFS as MP2 takes certain electron

Table 9. Electron density ϱ and Laplacian $\nabla^2\varrho$ (in a.u.) at the bond critical point. The distance r_c (in Å) is from the critical point to the first atom mentioned under 'bond'

Molecule	Bond		HF			MP2	HFS
			STO-3G	4-31G	6-31G**	6-31G**	TZD
Formaldehyde	C–O	r_c	0.392	0.412	0.391	0.398	0.429
		ϱ	0.341	0.389	0.413	0.415	0.416
		$\nabla^2\varrho$	1.454	0.171	0.601	0.312	−0.518
	C–H	r_c	0.633	0.682	0.675	0.682	0.708
		ϱ	0.265	0.272	0.305	0.301	0.279
		$\nabla^2\varrho$	−0.662	−0.846	−1.249	−1.189	−0.979
Water	O–H	r_c	0.729	0.743	0.771	0.765	0.748
		ϱ	0.379	0.347	0.377	0.373	0.348
		$\nabla^2\varrho$	−2.579	−1.650	−2.285	−2.115	−1.878
Nitrate	N–O	r_c	0.636	0.637	0.626	0.623	0.606
		ϱ	0.428	0.417	0.477	0.467	0.444
		$\nabla^2\varrho$	−0.823	−0.402	−1.006	−0.808	−0.647
Urea	C–O	r_c	0.407	0.435	0.402	0.410	0.450
		ϱ	0.356	0.396	0.415	0.415	0.408
		$\nabla^2\varrho$	0.421	−0.786	−0.200	−0.394	−0.880
	C–N	r_c	0.450	0.533	0.450	0.471	0.554
		ϱ	0.281	0.308	0.333	0.333	0.320
		$\nabla^2\varrho$	−0.069	−0.970	−0.978	−1.110	−0.889
	N–H1	r_c	0.699	0.741	0.759	0.756	0.736
		ϱ	0.341	0.332	0.362	0.357	0.339
		$\nabla^2\varrho$	−1.599	−1.592	−2.026	−1.941	−1.595
	N–H2	r_c	0.688	0.732	0.750	0.747	0.731
		ϱ	0.341	0.333	0.364	0.359	0.339
		$\nabla^2\varrho$	−1.505	−1.575	−2.013	−1.927	−1.552

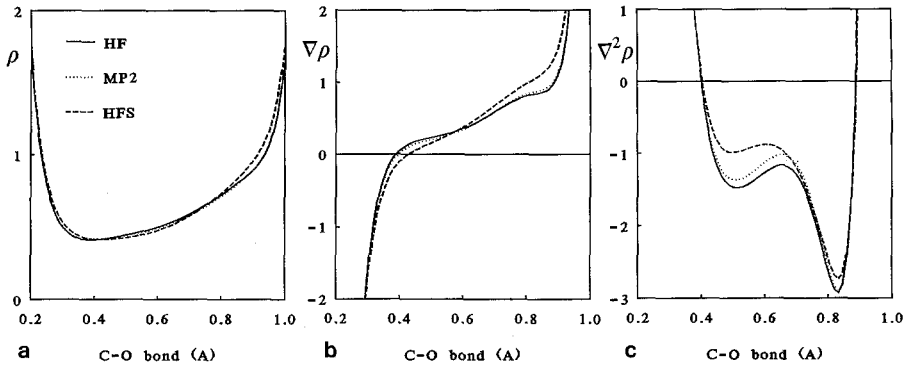

Fig. 7. Electron density ϱ (**a**), gradient of ϱ (**b**), and Laplacian $\nabla^2\varrho$ (**c**) along the C=O bond of formaldehyde calculated with HF/6-31g**, MP2/6-31g**, and HFS/TZD. The carbon atom is located at O. The critical point in this bond is located at 0.41 Å

correlation effects into account. The Laplacian $\nabla^2\varrho(r_c)$ depends quite strongly on the basis set used and sometimes even positive values were found, characteristic for closed-shell and ionic interactions. The bonds in these molecules should correspond to bonds with shared interactions ($\nabla^2\varrho < 0$), but basis set inadequacies apparently strongly influence the Laplacian. The Laplacian calculated with the HFS method is for all bonds negative as expected.

Figure 7 shows the sensitivity of the Laplacian for small changes in $\varrho(r)$ of the C=O bond of formaldehyde. Close to the critical point ($\sim$0.41 Å from the cabon atom) the graphs of $\nabla^2\varrho$, calculated with the HF, MP2, and HFS methods, almost coincide and the sign of $\nabla^2\varrho(r_c)$ depends on very small changes in the position of the critical point. Closer investigation of the different components of ϱ (the curvatures) shows that, at the critical point, the largest variations occur in the positive curvature, which is directed along the C=O bond. Since the density in this direction also determines the position of the critical point in the bond, small variations in ϱ can influence the position of the critical point and the magnitude of the Laplacian at this point. Although this behavior is not seen in all bonds and the Laplacian of ϱ is negative in a large part of the C=O bond of formaldehyde, we must be cautious with interpreting $\nabla^2\varrho$ at some specific point, as for example the (3, −1) critical point in the bond. Bader [25] classifies the C=O bond in formaldehyde as intermediate, since it doesn't really belong to one of the extreme cases, i.e. shared and closed-shell interactions.

3.4 (Hyper)polarizability of formaldehyde

The dipole moment μ, static dipole polarizability α and static first dipole hyperpolarizability β, have been calculated for formaldehyde and compared with experiments. The geometry used is in excellent agreement with the experimental geometry [57] which makes a direct comparison possible. For the calculations the sum over states (SOS) method and two finite field (FF) methods (see Sect. 2.6) have been used. One is based on the numerical differentiation of the dipole moment FF:μ (with respect to the electric field) while for the other the total energy is differentiated FF:E. For the HF calculation both FF methods should

yield the same values. For MP2 calculations both methods can yield different results, since the terms contributing to the dipole moment are different from those contributing to the energy.

From Tables 10, 11, and 12 can be seen that both FF methods indeed yield the same results for HF. The small differences for α and β are caused by inaccuracies in the numerical differentiation of the dipole moment and energy ($\Delta\alpha \leqslant 0.006$ a.u., $\Delta\beta \leqslant 0.4$ a.u.) The dipole moments, Tables 10 and 13, depend only slightly on the basis set, especially for the HFS method. Inclusion of polarization functions, contracted or diffuse, cause minor changes to the dipole moment. Incorporating electron correlation effects by MP2 is far more important. MP2 corrections cause a reduction of the HF dipole moments yielding values in excellent agreement with experiment. The HFS calculated dipole moments, Table 13, are lower than the MP2 values and also slightly lower than the experimental ones, but better than HF values. Considering the much larger computational effort needed for MP2 than for HFS the last method can be used as a powerful alternative. The *d*-polarization function gives a significant improvement to μ_{HFS} but basis sets larger than DZD yield the same values so that the basis set limit of α has probably been reached.

We now turn to the polarizability. Electron correlation does not seem to be important, in contrast with the results found the for dipole moment. The small 4-31G basis set (HF) yields already a very good value for α_{zz}, the polarizability along the molecular axis. Extending the basis with diffuse functions hardly changes this, but it does have a large effect on the other components of α. Along the main axis of the molecule, polarization has its main origin in a redistribution of charge over the atoms, while in the direction perpendicular to the molecular plane only atomic polarization contributes. The basis sets are obviously much more flexible in the molecular plane than perpendicular to it. The electron correlation contribution to the dipole moment, calculated by MP2, appears to be

Table 10. Dipole moment (in a.u.) of formaldehyde calculated with finite field methods based on the dipole moment derivative FF:μ and energy derivative FF:E

Basis set	HF FF:μ	FF:E	MP2 FF:μ	FF:E
STO-3G	−0.593	−0.593	−0.418	−0.477
4-31G	−1.188	−1.188	−0.923	−0.934
6-31G**	−1.095	−1.095	−0.858	−0.870
6-31G** + ext1[1]	−1.127	−1.127		−0.922
6-31G** + ext2	−1.127	−1.127		−0.922
6-31G** + ext3	−1.139			
TZV	−1.207			
TZV** + ext1	−1.136			
Experiment				−0.917[2], −920[3]

[1] Diffuse polarization functions: GTO's with the following types and exponents for the C, O, and H atoms (C and O)/(H):
- ext1 = ($\zeta_d = 0.2$, $\zeta_d = 0.05$)/($\zeta_p = 0.2$, $\zeta_d = 0.05$)
- ext2 = ext1 + ($\zeta_d = 0.005$)/($\zeta_d = 0.005$)
- ext3 = ext1 + ($\zeta_f = 0.1$)/-

[2] Ref. [50].
[3] Ref. [51].

Table 11. Static dipole polarizability α (in a.u.) of formaldehyde calculated with the sum over states (SOS) method and with finite field methods using HF and MP2 calculations. The C=O bond is directed along the z-axis, while the molecule is lying in the y-z plane. For specifications of the functions see Table 10

SOS	α_{xx}	α_{yy}	α_{zz}			
STO-3G	1.763	4.581	12.381			
4-31G	4.239	8.264	17.346			
6-31G**	6.596	9.969	16.770			
6-31G** + ext1	11.266	12.829	18.073			
6-31G** + ext2	11.356	12.850	18.098			
TZV	5.435	8.903	18.482			
TZV** + ext1	11.513	12.846	18.200			
	FF:μ			FF:E		
HF	α_{xx}	α_{yy}	α_{zz}	α_{xx}	α_{yy}	α_{zz}
STO-3G	2.444	5.730	10.231	2.444	5.730	10.232
4-31G	5.181	11.209	18.232	5.181	11.208	18.232
6-31G**	6.743	12.647	18.122	6.744	12.646	18.123
6-31G** + ext1	11.913	15.716	20.671	11.918	15.710	20.667
6-31G** + ext2	12.044	15.740	20.705	12.040	15.735	20.701
6-31G** + ext3						21.057
MP2						
STO-3G	2.441	5.789	8.599	2.418	5.775	8.606
4-31G	5.298	11.722	17.712	5.298	12.041	17.128
6-31G**	6.745	13.015	18.170	6.733	13.246	17.651
6-31G** + ext1				12.442	17.341	21.459
6-31G** + ext2				12.563	17.370	21.498
Experiment[1]				12.4	18.6	18.6
Experiment[2]				12.95	18.63	18.63

[1] Ref. [59] and [60].
[2] Ref. [61].

almost independent of the electric field resulting in only minor effects on the polarizability. The largest calculation, MP2(6-31G** + ext2), yields values for α in excellent agreement with experiments, with only the α_{zz} values being slightly too large. Raeymaekers et al. [58] analyzed different calculations of α and found that almost all α_{zz} values were calculated somewhat larger than the experimental values. Our calculation of α_{yy} (in the molecular plane, perpendicular to the molecular axis) is closer to the experiment than any of the other calculations, which are all too small. The SOS calculations yield quite good results for α_{xx} and α_{zz}, with only α_{yy} being clearly too small. The HFS calculations show a slight basis set dependence for all components of α. Diffuse polarization functions are not as important as for the HF and MP2 methods. The values are larger than for the HF calculation but in good agreement with experiments, with only α_{zz} being too large.

As a last point we discuss the hyperpolarizability of formaldehyde. We first discuss the outcome of the HF calculations and then the improvements by MP2

Table 12. Static first dipole hyperpolarizability β (in a.u.) of formaldehyde calculated with the (SOS) method and FF methods (HF and MP2). For specifications of the functions see Tables 10 and 11. $\beta_z = \beta_{xxz} + \beta_{yyz} + \beta_{zzz}$

SOS	β_{xxz}	β_{yyz}	β_{zzz}	β_z				
STO-3G	0.115	3.250	8.082	11.447				
4-31G	2.192	12.905	31.924	47.021				
6-31G**	2.091	11.134	27.821	41.046				
6-31G** + ext	14.978	10.324	31.211	46.513				
6-31G** + ext2	5.087	10.432	31.191	46.710				
TZV	4.000	11.711	32.260	47.971				
TZV** + ext1	5.047	10.128	30.982	46.157				
	FF: μ				FF: E			
HF	β_{xxz}	β_{yyz}	β_{zzz}	β_z	β_{xxz}	β_{yyz}	β_{zzz}	β_z
STO-3G	0.8	2.2	2.3	5.3	0.6	2.5	2.2	5.3
4-31G	3.0	19.5	19.5	42.0	2.8	19.8	19.2	41.8
6-31G**	1.9	17.7	19.3	38.9	1.6	18.1	19.1	38.8
6-31G** + ext1	3.6	13.2	19.5	36.3	3.4	13.4	19.5	36.3
6-31G** + ext2	3.6	13.3	19.3	36.2	3.4	13.5	19.3	26.2
6-31G** + ext3							18.1	
MP2								
STO-3G	0.6	3.7	−2.5	1.8	0.1	4.0	−1.3	2.8
4-31G	2.1	26.5	7.4	36.0	1.2	27.5	6.1	34.8
6-31G**	1.1	22.4	10.3	33.8	0.5	23.6	8.1	32.2
6-31G** + ext1					1.8	20.0	12.3	34.1
6-31G** + ext2					1.6	20.1	12.0	33.7

corrections. The SOS calculation of β_{zzz} yields larger values than the FF calculations, for all basis sets. The agreement between both methods is closer for the components β_{xxz} and β_{yyz}. Because of the numerical integration in the HFS method the dipole moment cannot be determined with greater accuracy than 10^{-4} a.u. making a reliable calculation of β not possible.

The static first dipole hyperpolarizability β behaves opposite to α with respect to electron correlation effects. As for the dipole moment, electron correlation is important for all components of β. For β_{zzz} it is more important to incorporate electron correlation effects than extending the basis set, while for β_{yyz} MP2 corrections and basis set extensions yield equal but opposite contributions. It is remarkable that for the HF calculations β_{zzz} is the largest component while for MP2 the largest value is found for β_{yyz}. The result of this difference in behavior of β_{yyz} and β_{zzz} with respect to the basis set size and electron correlation effects is that the experimental measurable quantity β_z ($=\beta_{xxz} + \beta_{yyz} + \beta_{zzz}$) is almost the same for all calculations.

Our calculations agree with one of the few reported values [59] of β calculated with the HF-FF method $\beta_{xxz} = 4.10$ a.u., $\beta_{yyz} = 16.20$ a.u. and $\beta_{zzz} = 20.19$ a.u.

For all calculations we have seen that MP2 gives almost the same results for both FF methods: the differences are usually small compared with the total

Table 13. Dipole moment μ and static dipole polarizability α of formaldehyde calculated with the HFS method using the finite field approach FF: μ. For the orientation of the molecule see Table 11. All electron calculation, no frozen core

Basis set	μ_z	α_{xx}	α_{yy}	α_{zz}
SZV	−0.164	5.462	17.758	16.835
DZV	−1.010	7.206	13.783	19.710
DZD	−0.876	11.586	17.049	20.479
TZD	−0.875	11.271	17.124	22.257
TZDF	−0.880	11.955	17.845	22.680
TZD + ext4[1]	−0.868	13.018	19.222	23.422
TZD + ext5	−0.889	13.975	20.039	24.353
TZDF + ext5	−0.875	13.996	19.859	24.193

[1] Diffuse polarization functions: STO's with the following types and exponents for the C, O, and H atoms (C, O)/(H):
- ext4 = $(\zeta_d = 0.5)/(\zeta_p = 0.5)$
- ext5 = ext4 + $(\zeta_d = 1.0)/(\zeta_p = 1.0)$

electron correlation effect. The difference between both methods has also been discussed in another paper [49].

4 Conclusions

From the analysis of the results obtained by the various quantum chemical methods we conclude that:

The electron density distributions obtained by the HF and HFS methods are in good agreement while electron correlation effects are relatively small. The differences in the densities between the HF and HFS methods shows electron correlation effects which are qualitatively in reasonable agreement with MP2 calculations.

The Hirshfeld stockholder method has been found more suited for comparing electron density distributions than the Mulliken, Löwdin, and Bader partitioning method, since it is less basis set dependent. Although the MP2 contribution to the density plots is relatively small it has a large effect on atomic charges resulting in an excellent agreement with the HFS charges. This clearly illustrates that the HFS method does include electron correlation effects and yields results of better quality than the Hartree–Fock method.

The electron densities at the bond critical points calculated with the HF method is in reasonable agreement with the HFS calculations. The agreement is slightly increased taking electron correlation (MP2) into account.

The HFS dipole moment of formaldehyde, urea, and water agree better with experiment than the HF value. Performing an MP2 calculation improves the HF values considerably yielding excellent agreement with experiments.

All methods yield good results for the polarizability of formaldehyde. The influence of electron correlation is much larger for the first hyperpolarizability than for the polarizability. Interesting is that basis set and electron correlation effects on the different tensor components of β tend to cancel each other resulting in a consistent behavior of the β_z with increasing basis set.

We conclude that the HF and HFS method give comparable electron density distributions but that agreement increases considerably using MP2. Since the last method is computationally much more demanding, the HFS method is a good alternative to perform calculations beyond Hartree–Fock.

References

1. Cook M, Karplus M (1987) J Phys Chem 91:31
2. Dreizler RM, Gross EKV (1990) Density functional theory. Springer-Verlag, Berlin
3. Hohenberg P, Kohn W (1964) Phys Rev B 136:864
4. Kohn W, Sham LJ (1965) Phys Rev 140:A1133
5. Baerends EJ, Ellis DE, Ros P (1973) Chem Phys 2:41
6. Baerends EJ, Ros P (1973) Chem Phys 2:52
7. Ellis DE, Painter GS (1970) Phys Rev B 2:2887
8. Painter GS, Ellis DE (1970) Phys Rev B 1:4747
9. Boerrigter PM, te Velde G, Baerends EJ (1988) Int J Quant Chem 33:87
10. Löwdin PO (1959) Adv Chem Phys 2:207
11. Wilson S (1984) Electron correlation in molecules. Clarendon Press, Oxford
12. Wilson S (1987) Electron correlation in atoms and molecules. Plenum Press, NY
13. Feil D, Uiterwijk J (1988) Portgal Phys 19:397
14. Møller C, Plesset MS (1934) Phys Rev 46:618
15. Wang LC, Boyd RJ (1989) J Chem Phys 90:1083
16. Boyd RS, Wang LC (1989) J Comput Chem 10:376
17. Dupuis M, Spangler D, Wendoloski JJ (1980) NRCC Software Catalog, vol 1 Program N. QG01 (GAMESS); Guest MF, Kendrick J (1985) GAMESS Users Manual, Daresbury Lab
18. Dupuis M, Spangler D, Wendoloski JJ (1980), NRCC Software Catalog, vol 1 Program N. QG01 (GAMESS); Schmidt MW, Baldridge KK, Boatz JA, Jensen JH, Koseki S, Gordon MS, Nguyen KA, Windus TL, Elbert ST (1990) QPCE Bulletin 10:52–54
19. Hall GG (1985) Adv Atomic Mol Phys 20:41
20. Mulliken RS (1955) J Chem Phys 23:1833, 23:1841, 23:2338, 23:2343
21. Huzinaga S, Sakai Y, Miyoshi E, Narita S (1990) J Chem Phys 93:3319
22. Löwdin PO (1950) J Chem Phys 18:365
23. Hirshfeld FL (1977) Theor Chim Acta 44:129
24. Davidson ER, Chakravorty S (1992) Theor Chim Acta 83:319
25. Bader RFW (1990) Atoms in molecules – A quantum theory. Clarendon Press, Oxford
26. Bader RFW, Essén H (1984) J Chem Phys 80:1943
27. Biegler-König FW, Nguyen-Dang TT, Tal Y, Bader RFW, Duke AJ (1981) J Phys B 14:2739
28. Biegler-König FW, Bader RFW, Ting-Hua Tang (1982) J Comput Chem 3:317
29. Velders GJM, Gillet JM, Becker PJ, Feil D (1991) J Phys Chem 95:8601
30. Chemla DS, Zyss J (1987) (Eds). Nonlinear optical properties of organic molecules and crystals, Vol 1 and 2, Academic Press, NY
31. Szabo A, Ostlund NS (1989) Modern quantum chemistry. McGraw-Hill, NY
32. Cohen HD, Roothaan CCJ (1965) J Chem Phys 43:S34
33. Cohen HD (1965) J Chem Phys 43:3558
34. Caves TC, Karplus M (1969) J Chem Phys 50:3649
35. Nakatsuji H, Musher JI (1974) J Chem Phys 61:3737
36. Hariharan PC, Pople JA (1972) Chem Phys Lett 66:217
37. Binkley JS, Pople JA (1977) J Chem Phys 66:879
38. Francl MM, Pietro WJ, Hehre WJ, Binkley JS, Gordon MS, DeFrees DJ, Pople JA (1982) J Chem Phys 77:3654
39. Hehre WJ, Ditchfield R, Pople JA (1972) J Chem Phys 56:2257
40. Dunning TH, Hay PJ (1987) In: Schaefer III HF (ed) Methods of electronic structure theory, Chap 1, Plenum Press, NY
41. Feller D, Davidson ER (1990) In: Lipkowitz KB, Boyd DB (eds) Reviews in computational chemistry, Chap 1, VCH Publ, NY

42. Snijders JG, Baerends EJ, Vernooijs P (1981) At Data Nucl Data Tables 26:483
43. Cade PE, Huo WM (1967) J Chem Phys 47:614
44. McLean AD, Yoshimine M (1967) Tables of linear molecule wavefunctions. IBM, NY
45. Bicerano J, Marynick DS, Lipscomb WN (1978) J Am Chem Soc 100:732
46. Davidson ER, Feller D (1986) Chem Rev 86:681
47. Benedict WS, Gailar N, Plyler EK (1956) J Chem Phys 24:1139
48. Meyer H, Schweig A, Zittlau W (1982) Chem Phys Lett 92:637
49. Velders GJM, Feil D (1992) J Phys Chem 96:10725
50. Fabricant B, Krieger D, Muenter JS (1977) J Chem Phys 67:1576
51. Starck B (1967) In: Hellwege (ed) Landolt–Bornstein: Molecular constants from microwave spectroscopy, vol 4, Springer Verlag, Berlin
52. Dyke TR, Muenter JS (1973) J Chem Phys 59:3125
53. Kirchhoff WH, Lide DR (1967) Natl Stand Ref Data Ser Natl Bur Stand 10
54. Clough SA, Beers Y, Klein GP, Rothman LS (1973) J Chem Phys 59:2254
55. Brown RD, Godfrey PD, Storey J (1975) J Mol Spectrosc 58:445
56. Krijn MPCM, Feil D (1986) J Chem Phys 85:319
57. Tanaka Y, Machida K (1977) J Mol Spectrosc 64:429
58. Raeymaekers P, Figeys HP, Geerlings P (1988) Mol Phys 65:945
59. Fowler PW (1982) Mol Phys 47:355
60. Timmermans J (1960) The physico-chemical constants of binary systems in concentrated solutions. Wiley Interscience, NY
61. Applequist J, Carl JR, Fung KK (1972) J Am Chem Soc 94:2952